Research and Reviews: Journal of Engineering and Technology
e-ISSN: 2347-226X
p-ISSN: 2319-9857

Synthesis of Spinel Ferrite with their Magnetic Properties, Reusability, Particle Size, Fuels, Surface Area, Dye Degradation as Application

Rahul Jarariya*

Department of Chemical Engineering, Vishwakarma Government Engineering College, Chandkheda, Gujarat, India

Mini Review

Received: 11-Jan-2022, Manuscript No. JET-22-52616; **Editor assigned:** 13-Jan -2022, Pre QC No. JET-22-52616 (PQ); **Reviewed:** 27-Jan -2022, QC No. JET-22-52616; **Accepted:** 31-Jan -2022, Manuscript No. JET-22-52616 (A); **Published:** 07-Feb -2022, DOI: 10.4172/ 2319-9865.11.2.002.

***For Correspondence:**
Rahul Jarariya, Department of Chemical Engineering, Vishwakarma Government Engineering College, Chandkheda, Gujarat, India

E-mail: rudrakashj47@gmail.com

Keywords: Microwave solution combustion method; Ferrites; Spinels; Doped spinels; Dyes

Abstract

Ferrite spinel gained huge attention due to its wide application area from biomedical to wastewater treatment, pharmaceuticals, biomedical, electronic devices, photocatalyst etc. The common ferrite spinal formula is M-Fe_2O_4 where M is Fe, Co, Mn, Zn, Cu, and Ni. The Microwave Solution Combustion (MSC) method and Solution Combustion Synthesis (SCS) is promising methods for catalytic activity or any solid material. This method is fast, energy-efficient and needs lesser equipment than any others. MSC method is reviewed in detail with insight into the effect of parameters. In this process, microwave irradiation is used to keep precursors at an excited state and make them highly reactive. Normally 2.45 GHz frequency microwave is used for this process. As this process is a solvent-free process. The most commonly used metal sources are nitrates of metals and fuel precursors are urea, L-arginine, glycerol etc. Urea is the most commonly used fuel because it gives less particle size. Different parameters such as fuel to oxidizer ratio, irradiation time, power of microwave and temperature and pressure can be optimized to get faster and better yield. This process does not need further calcination but needs several items of washing with ethanol or n-butanol for purification of the final product. In the end, it generates a large volume of gases produced during the combustion process. And this process can be used only for laboratory purposes till yet and some research is awaited on rare earth metals doped with spinel. But in SCS, directly jump to calcination after precursor homogenized at neutral pH i.e., 7. Both methods can work collimated if required a higher degree of separation with better yield and magnetic separation susceptibility during implementation on degradation on dye.

INTRODUCTION

Spinel can be synthesis by sol-gel, co-precipitation, microemulsion, solid-state, Hammer's method, microwave combustion method, sol-gel auto combustion method, solution combustion method etc. Microwave solution method overcome from other methods because its efficient, time-saving, fast route for preparing spinel ferrites and doping of spinel ferrite also going to new generation catalyst for dye degradation as application [1]. Spinel ferrites due to their outstanding magnetic and electrical properties or high chemical and thermal sjkoptabilities. Generally, Spinel ferrite is expressed as MFe_2O_4. Where M is known as Transition metals. It is kept voids between Tetrahedral and Octahedral containing A and B sites cations in spinel ferrite structure. Here, in Inverse spinel kept Iron (III) trivalent cation fixed and other divalent cation can be arranged as per requirement. It is widely reported that the magnetic, electrical and chemical properties of nanocrystalline ferrites are very sensitive to processing techniques. The inversion parameter and magnetic are strongly dependent upon size, shape, stoichiometry, crystalline, and surface groups all of which are also controlled by preparation and post preparation methods.

Solution combustion synthesis also synthesized and increased production of ferrites due to its magnetic properties and possibility of producing highly pure and homogenous structure powered and low cost, short times. SCS is also called another route to processed ferrites. It consists of a combination of both oxidizer and fuel ration for combustion in the aqueous medium [2]. The mixture is heated up until it reaches self-sustaining ignition is fast and highly exothermic combustion. The precursor solution is then combusted by extra heating up to the mean temperature (200-500˚C) to form the final product directly. Sometimes, it is required to calcine the combusted products at higher temperatures (<700˚C). The catalyst powder is strongly dependent upon the F/O ratio. The F/O ratio maintained is equal to 1. The powder amount is the crucial factor for turning the phase and microstructured combusted powders. Here, this paper reviewed both on Microwave solution combustion synthesis and Solution Combustion Synthesis (SCS) method (Figure 1).

Figure 1. Microwave solution combustion synthesis and Solution Combustion Synthesis (SCS) method.

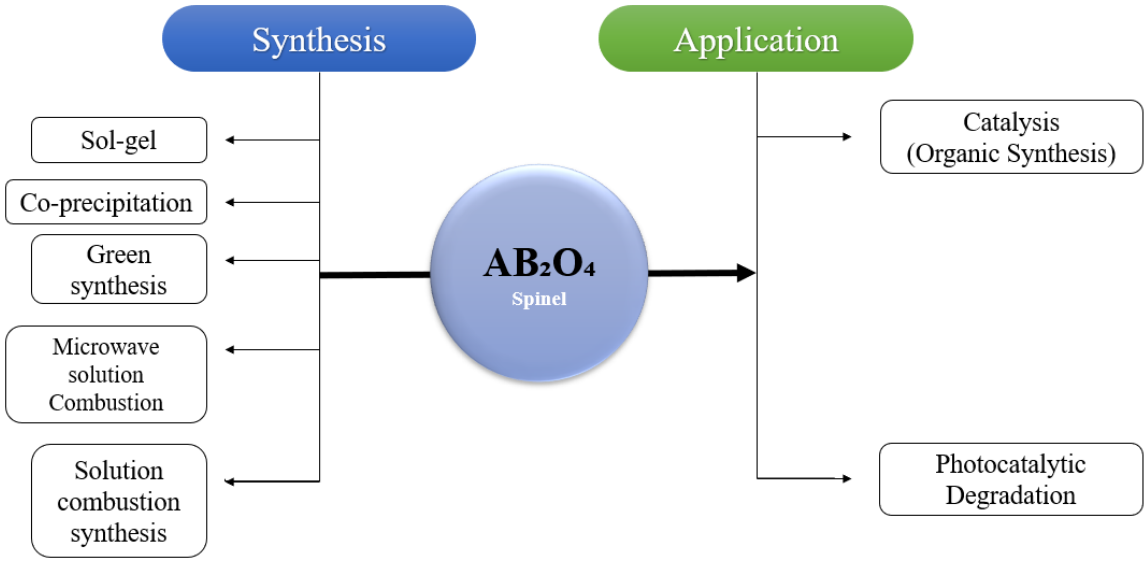

Spinel ferrite can be utilized for dye degradation from wastewater. The dyeing and textile industry is responsible for dye discharge as well as a plethora of other hazardous substances (either inorganic or organic). The dye wastewater causes several effects on the environment. It causes asthma problems, carcinogenic diseases, skin irritation, eyesight problems, and many others. The problem of dye contaminated water is especially evident in Asia,

which contributes about 50% of textile exports and more than 50% of the world's consumption of dyes. Only discharged water needs to degrade. The quality of wastewater has already been announced as per CBCP (Central Pollution Control Board) and GCPC (Gujarat Pollution Control Board).

The majority of industrial dyes and impacted into the environment such dyes are Azo dyes, Reactive dyes, Anthraquinone dyes, Acidic and basic dyes. Azo make up over 60% of the synthetic dyes used industrially followed by other dyes. Azo (Reactive dyes) are easily available at a cheap cost [3]. Its stability in water is high. Dye the chromophore group (-N=N-) linkages. And sulphonic group present in (SO^{3-}) in reactive dyes (Table 1).

Table 1. The types of Reactive dye.

Categories of reactive dyes
Reactive turquoise Blue H5G
Reactive Navy Blue HE2R
Reactive Blue 171
Reactive Turquoise Blue MGN
Reactive Red Brown
Reactive yellow
Reactive Purple
Congo Red reactive dyes
Reactive orange dyes etc.

MICROWAVE SOLUTION COMBUSTION METHOD

Microwave chemistry

1. Inside the strong metal box, there is a microwave generator called a magnetron. When you start cooking the magnetron takes electricity from the power outlet and covers it into high-powdered, 12 cm (4.7 in) radio waves.
2. The magnetron blasts these waves into the food compartment through a channel called a waveguide.
3. The food sits on a turntable, spinning slowly round so the microwaves cook it evenly.
4. The microwaves bound back and forth off the reflective metal walls of the food compartments, just like light bounces they not simply bound off. Just as radio waves can pass straight through the walls of your house, microwaves penetrate inside the food. As they travel through it, they make the molecule inside it vibrate more quickly.
5. Vibrating molecules have heat so, the faster the molecules, the hotter the food becomes. Thus, the microwaves pass their energy onto the molecules in the food, rapidly heating it. The only loss factor in the microwave is energy loss in a dielectric material due to slow polarization or some other dissipative phenomenon.

Muffle furnace

It is the equipment for heating or combustion of the material significantly in high temperature while keeping it contained chemicals or other substances. It is usually lined with stainless steel, making them largely corrosive. Different samples were heated in the furnace around 400˚C-2000˚C. Depending on the size of the muffle and various requirements in heating elements (Kanthal resistive wire, Silicon carbide rods, Molybdenum Disilicate) for a higher temperature around <1500˚C. PID based controller arranged in a muffle furnace [4]. The controller is set out

by set value and Process Value (PV). A high-density ceramic fibre blanket is used as insulation to keep the outer surface at minimum temperature (Table 2).

Table 2. Basic specification of muffle furnace.

Max temperature	1100˚C	1400˚C
Continuous operating temp	1000˚C	1300˚C
Heating element	Kanthal wire	Silicon carbide (SiC) rods
Thermocouple	K Type	R Type
Chamber MOC	Ceramic fibreboard	Ceramic Zirconium board
Exterior MOC	Mild steel powder-coated	Mild steel powder-coated
Insulation	Ceramic fibre blanket	Ceramic fibre blanket
Temperature controller	PID controller with SCR power control	PID controller with SCR power control
Power supply	220 Volts 50 Hz	3 Phase 440 Volts 50 Hz (with energy-saving transformer assembly)
Accessories	One pair of furnace gloves	
	One crucible steel tong	
Optional	Exterior made of SS 304 / SS316 (GMP model)	
	30 Segment profile controller for heating and cooling rate	
	PLC with Color HMI (data logging and USB Interface)	
	RS485 with PC interface	
	Data logger with PC/USB interface	
	Calibration certificate	
	Door safety switch	
	Silicon carbide bottom plate	
	Caster wheels with brake	

Hot plate

The hot plate is generally used for combustion synthesis with chemical propellants. Many researchers worked in an inexpensive way to generate high conversion degree catalysts with this equipment. A hot plate can have a flat surface around or around the surface; this part is used for heating purposes to heat the beaker with the mixture inside it [5]. The operating temperatures vary from 100 to 750˚C with 120 to 148 Voltage range.

Procedure for experiments

Required amounts of iron nitrate $Fe(NO_3)_3.9H_2O$, mixture with divalent metal cation with fuel consisted reducing agent and is also capable for the combustion reaction. Then proceed to make propellent dissolved in distilled water for solubilizing. Only for the mixture of fuels, the pH of the solution precursor was adjusted to 7 with the addition of ammonia solution (NH_4OH) under continuous stirring. The mixture slowly evaporated at 80˚C until a viscous solution was formed. The mixture was poured into a round bottom flask and heated until it transformed into a gel;

e-ISSN: 2347-226X
p-ISSN: 2319-9857

by further heating up to 250˚C, the ignition reaction started from a point and propagated spontaneously. The combustion gases were bubbled in a large beaker filled with water. The obtained powders by hand-crushed with a pestle (Figure 2).

Figure 2. Microwave solution combustion method with dye degradation.

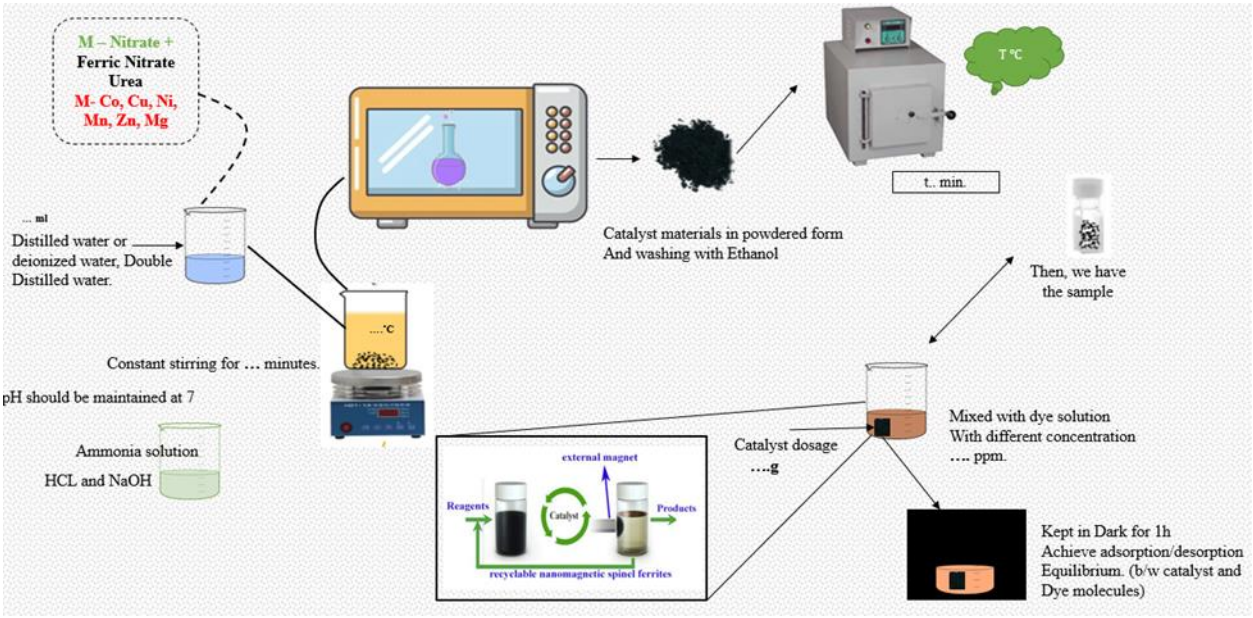

The procedure of solution combustion synthesis experiment

The various amounts of fuels with the precursors dissolved in distilled water. Normally we can take 30 ml, 50 ml depending on the amount of material to be made. The combustion gaseous product was considered as CO_2, H_2O, and N_2. But it depends on the combustion temperature. After the process proceed for reaction F/O ratio equalized to 1 but sometimes 1.5 or >1 respectively. A brown dried gel combusted in the semi-closed system or can use types of muffle furnace for combustion [6,7]. The temperature can be determined by TGA/DSC analysis (thermal deposition of powder). It can be 500˚C, 600˚C, 700˚C-1000˚C. Then, dried powdered crushed by mortar with pestle (Figure 3).

e-ISSN: 2347-226X
p-ISSN: 2319-9857

Figure 3. Solution combustion method with dye degradation.

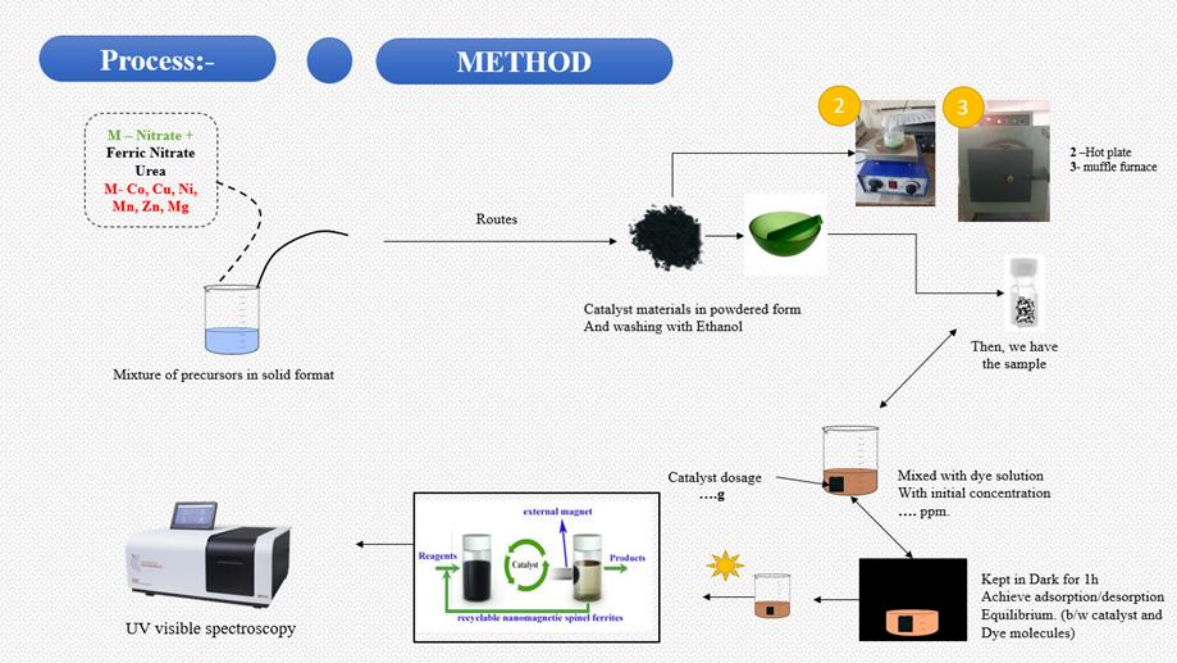

PHOTOCATALYSIS

The activity can be implemented with UV light or visible light be seen in our study. This PCA has been seen with Methylene dyes, Reactive turquoise blue-21 dyes, Methyl orange, Congo red, Reactive red-141 etc. Believe me, these dyes degraded with maximum efficiency with the help of a catalyst [8,9]. The catalyst dissolved in an aqueous solution to achieve sonication with respective time either it would be 10 min or more. Then, the sample is kept in a dark room at room temperature with constant stirring until adsorption/desorption equilibrium. Sample to dark stirring was collected and analyzed to get spectra [10,11]. In UV light, the samples were collected at different time intervals (Figure 4). This experiment can use the beaker (borosilicate glass). pH should be adjusted and proceed for calculation (Table 3).

$$\text{Degradation of dye } (\%) = [(C_0 - C_i)/C_0] \times 100$$

Where, C0 and Ci are the initial concentration and final concentration with different time intervals, respectively.

Figure 4. Photocatalyst in visible source with reaction mechanisms.

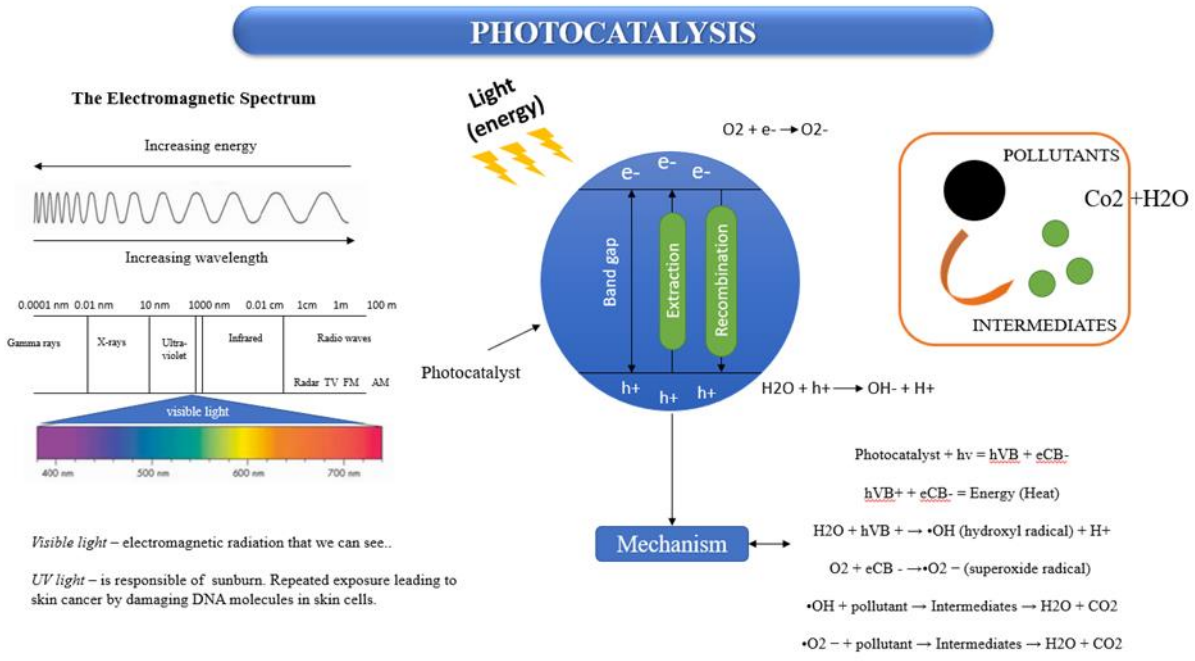

Table 3. Different dye degradation with suitable material.

Materials	Dyes	Degradation efficiency	Irradiation time (min.)	Light source	References
$CuFe_2O_4$	Methylene Blue	94%	105	125 W Hg lamp (UV light)	M.A. Shilpa Amulya, et al.
$Ni_{0.8}Zn_{0.2}Fe_2O_4$	Rhodamine B	98.48%	120	Visible light	A. Jadhav, et al.
$Zn:CuFe_2O_4$	Direct Red 264	55%	120	Xenon lamp (Visible light)	S.Anandan, et al.
$Ag:CuFe_2O_4$	Malachite Green	98%	240	UV light	M.A. Shilpa Amulya, et al.
$Ti:CuFe_2O_4$	Methylene Blue	82%	180	500 W Xenon lamp (Visible light)	M Kamel Attar Kar, et al.
$CuFe_2O_4/Bi_2O_3$	Methylene Blue	90%	45	Sodium lamp (Visible light)	Surendra, et al.
$CuFe_2O_4/rGO$	Phenol	90%	180	400 W Xenon lamp (Visible light)	Arifin, et al.

CHARACTERIZATION

FTIR measurement

Degraded dye products were collected after colour removal reaction by centrifugation and vacuum dried. The IR spectra of dye and degraded dye product after the decolourization procedure can be recorded in FTIR: 4000-400 cm^{-1} range. FTIR spectra give a reasonable hint of the modifications happening in a dye molecule because of decolourization as a result of the vanishing of existing peaks. Thus, the degradation of dye by NPs included the simultaneous adsorption and catalytic of dye occurring on NPs [12,13].

XRD

Structural configuration, crystallize size, space group. The crystallite size was calculated employing the Scherrer formula. If the crystalline size is decreased also enhances the large surface area. The prepared sample was formed with cubic phase with face-centred lattice and it shows Fd_3m space group. The study defines the intensity of the peaks differs which exhibits the tough crystallization because of the large radii of it using rare earth metals which has been used for doping. XRD patterns confirm the formation of a single-phase spinel catalyst without impurities. The average crystallite size (D) was calculated using Debye Scherrer's formula.

The breadth of the Bragg peak is the combination of both instrument and sample broadening effects. Hence, the line broadening due to the instrument has to be decoupled with that of the sample by recording the diffraction pattern and studying the line broadening of standard material such as silicon [14,15]. The instrument corrected broadening; b corresponding to the diffraction peak of zinc aluminates was estimated using relation.

$$D=(0.9\ \lambda)/(\beta \cos \theta)$$

The effective particle size (D) and the strain component were also evaluated using Williamson-Hall method. If the slope shows negativity, it means the compressive strain, whereas the appearance of a positive slope indicates the possibility of tensile strain. In the present study, a positive slope for all the samples reveals the presence of tensile strain in the composites. The X-ray density (dx) for each sample was calculated by the relation [16,17].

$$Dx=ZM/NV$$

Where Z is the number of molecules per unit cell of spinel lattice (Z=8), M is the molecular weight, V is the unit cell volume, and N the Avogadro's number.

The percentage porosity (P) of the spinel was calculated by using the formula

$$P=1-[\text{Bulk density}/\text{X ray density}]*100$$

The reduction in bandgap energy will make the catalyst capable of having efficiency in visible light which is present largely in solar light and can give good photocatalytic efficiency.

The vibrational, rotational and lattice defects present on the samples were found by Raman analysis [18,19].

Scanning electron microscopy

Morphological, development of clear nanoparticles with size reduction is also evident from the image. The particles at the 500 nm scale show better-grown nanoparticles with less agglomeration on the surface of the grown nanoparticles. While doping agglomeration completely reduced the nanoparticles grown and more clear surfaces. At the 500 nm scale, the image will clear support [20,21].

EDAX

It confirms the elemental configuration.

Thermal Gravimetric Analysis (TGA)

It is widely used to investigate the thermal decomposition of NPs to determine the thermal decomposition kinetic parameter. These parameters can be used to obtain a better understanding of the thermal stability of the catalyst.

Magnetization

The magnetization behaviour of catalyst or doped catalyst can be investigated with VSM (Vibrational Sample Magnetometry) by seeping the external magnetic field. Magnetization plotted against, applied field (H) behaviour plots. The values of coercivity and retentivity obtained from the M-H curves, the low values are attributed to the characteristic of magnetic NPs where thermal fluctuations are sufficient to overcome the anisotropy energy barrier, thus allowing the magnetization to spontaneously reverse the direction, Upon increasing the amount of doping as tends to super magnetization behaviour, However, increase in the doping concentration by a decrease in the coercivity value decreased due to the thermal fluctuations can be, it assisting the overcoming of anisotropy energy barrier. The smaller values of squareness ratio Mr/Ms less than 0.5, according to stoner wolfarth indicate the nanoparticles process uniaxial anisotropy. The squareness ratio classifies the materials to have cubic anisotropy [22,23]. The magnetocrystalline anisotropy constant (K) of the NPs obeying uniaxial anisotropy is calculated using Brown's relation (Table 4).

K1=(Hc Ms)/0.985

It has been observed that the anisotropy constant (k1) decreases at higher calculations temperature (˚C).

Table 4. Literature survey on spinel's Magnetization properties with different fuels.

Catalyst Name	Synthesis Methods	Fuel	Saturation magnetization (Ms)-emu/g	Remanence magnetization (Mr)-emu/g	Coercivity (Hc) (Oe)	References
$CoFe_2O_4$/RGO	Solvothermal synthesis	-	41.98	25.42	6.41	L Hu, et al.
$ZnSeWO_3eCoFe_2O_4$	Wet impregnation	-	0.6503	-	1000.03	Bharathi, et al.
Co-doped $ZnAl_2O_4$	Microwave combustion method	Glycine	-	0.23	217.39	G.T. Anand et al.
$Zn_{1-x}Co_xAl_2O_4$	Microwave-Assisted Combustion Method	Ethylenediaminetetraacetic acid	-	0.00137	52.25	Ramachandran et al.
8% Co-doped Fe_3O_4 NPs	Co-precipitation	-	29.51	6.48	308.14	A. Wahab, et al.
$MgFe_2O_4$ (glycine)	Solution combustion method	Urea	27	-	51	Masoudpanah, et al.
$NiFe_2O_4$	Solution combustion synthesis	Glycine	59	13	95	Martinson K.D, et al.
$CoFe_2O_4$, $Co_{0.5}M_{0.5}Fe_2O_4$ (M=Mn,Ni,Zn)	Solution combustion synthesis	Oxalyl di hydrazide	76.1	-	-	Bera, et al.
$Ni_{0.5}OCo_{0.5}OFe_2O_4$	Microwave combustion synthesis	Glycine	33.3	14.3	941	Freitas, et al.

CONCLUSION

Microwave solution combustion or solution combustion method both works collimated each other. The great propellent discovery found in the microwave and easy reaction with less contact time to produce a suitable catalyst for dye degradation. Our study shows microwave comes in viable synthesis method for NPs based catalyst but the drawback with a large number of gases produced (NOx, COx, NH_3 etc.) but it depends on the selected material for combustion and it is produced by exothermic reaction with as in $CoFe_2O_4$, $NiFe_2O_4$, $MgFe_2O_4$-spinel ferrites materials and its produce good magnetization for easy separation with dye (either reactive dyes or others).

Solution combustion assisted work the catalyst for reducing particle size with a certain amount to temperature (400-2000˚C) in muffle furnace during calcination and produce crucial separation. So, the microwave is a very effective work for dye degradation as an application.

REFERENCES

1. Hadadian S, et al. Solution combustion synthesis of Fe_3O_4 powders using mixture of CTAB and citric acid fuels. J Supercond Nov Magn. 2019;32:353-360.
2. Astaraki H, et al. Effects of fuel contents on physicochemical properties and photocatalytic activity of $CuFe_2O_4$ Reduced Graphene Oxide (RGO) nanocomposites synthesized by solution combustion method. J Mater Res Technol. 2020;9:13402-13410. [Crossref] [Google Scholar]
3. Martinson KD, et al. Synthesis of $Ni_{0.4}Zn_{0.6}Fe_2O_4$ spinel ferrite and microwave adsorption of related polymer composite. Nanosystems: physics, chemistry, mathematics. 2020;11. [Crossref] [Google Scholar]
4. Heidari P, et al. Structural and magnetic properties of $MgFe_2O_4$ powders synthesized by solution combustion method: the effect of fuel type. J Mater Res Technol. 2020;9:4469-4475. [Crossref] [Google Scholar]
5. Martinson KD, et al. Single-step solution-combustion synthesis of magnetically soft $NiFe_2O_4$ nanopowders with controllable parameters. Int J Self-Propagating High-Temp Synth. 2019;28:266-270.
6. Bera P, et al. Solution combustion synthesis, characterization, magnetic, and dielectric properties of $CoFe_2O_4$ and $Co_{0.5}M_{0.5}Fe_2O_4$ (M=Mn,Ni, and Zn). Phys Chem Chem Phys. 2020;22:20087-20106. [Crossref] [Google Scholar] [PubMed]
7. Nguyen LT, et al. A facile synthesis, characterization, and photocatalytic activity of magnesium ferrite nanoparticles via the solution combustion method. J Chem. 2019. [Crossref] [Google Scholar]
8. Habib IY, et al. Effect of Cr doping in CeO_2 nanostructures on photocatalysis and H2O2 assisted methylene blue dye degradation. Catalysis Today. 2021;375:506-513. [Crossref] [Google Scholar]
9. Keerthana SP, et al. Influence of tin (Sn) doping on Co_3O_4 for enhanced photocatalytic dye degradation. Chemosphere. 2021;277:130325. [Crossref] [Google Scholar]
10. Rambabu K, et al. Green synthesis of zinc oxide nanoparticles using Phoenix dactylifera waste as bioreductant for effective dye degradation and antibacterial performance in wastewater treatment. J Hazard Mater. 2021;402:123560. [Crossref] [Google Scholar] [PubMed]
11. Zhang J, et al. Visible-light photo-Fenton catalytic MgFe2O4 spinel: Reaction sintering synthesis and DFT study. J Alloys Compd. 2022;889:161673. [Crossref] [Google Scholar]

12. Vijayaraghavan T, et al. Visible light active $LaFeO_3$ nano perovskite-RGO-NiO composite for efficient H_2 evolution by photocatalytic water splitting and textile dye degradation. J Environ Chem Eng. 2021;9:104675 [Crossref] [Google Scholar]

13. Katoch V, et al. Microflow synthesis and enhanced photocatalytic dye degradation performance of antibacterial Bi 2 O 3 nanoparticles. Environ Sci Pollut R. 2021;28:19155-19165. [Crossrefer] [Google Scholar] [PubMed]

14. Mishra S, et al. Cobalt ferrite nanoparticles prepared by microwave hydrothermal synthesis and adsorption efficiency for organic dyes: isotherms, thermodynamics and kinetic studies. Adv Powder Technol. 2020;31:4552-4562. [Crossref] [Google Scholar]

15. Vasantharaj S, et al. Synthesis of ecofriendly copper oxide nanoparticles for fabrication over textile fabrics: characterization of antibacterial activity and dye degradation potential. J Photochem Photobiol. 2019;191:143-149. [Crossref] [Google Scholar] [PubMed]

16. Naik MM, et al. Green synthesis of zinc doped cobalt ferrite nanoparticles: Structural, optical, photocatalytic and antibacterial studies. Nano-Struct. Nano-Objects. 2019;19:100322 [Crossref] [Google Scholar]

17. Kafshgari LA, et al. Synthesis and characterization of manganese ferrite nanostructure by co-precipitation, sol-gel, and hydrothermal methods. Part Sci Technol. 2018;37:904-907. [Crossref] [Google Scholar]

18. Moradnia F, et al. Green synthesis of recyclable MgFeCr04 spinel nanoparticles for rapid photodegradation of direct black 122 dyes. J Photochem Photobiol. 2020;392:112433 [Crossref] [Google Scholar] [PubMed]

19. Iqbal M, et al. Microwave assisted synthesis of zinc vanadate nanoparticles and photocatalytic application. Mater Res Express. 2020; 7:015070. [Crossref] [Google Scholar] [PubMed]

20. Atrak K, et al. Green synthesis of Zn0. 5Ni0. 5AlFe04 magnetic nanoparticles and investigation of their photocatalytic activity for degradation of reactive blue 21 dye. Environ Technol. 2020;41:2760-2770. [Crossref] [Google Scholar] [PubMed]

21. Borade RM, et al. Spinel zinc ferrite nanoparticles: an active nanocatalyst for microwave irradiated solvent free synthesis of chalcones. Mater Res Express. 2020;7:016116. [Crossref] [Google Scholar] [PubMed]

22. Kafshgari LA, et al. Synthesis and characterization of manganese ferrite nanostructure by co-precipitation, sol-gel, and hydrothermal methods. Part Sci Technol. 2018;37:904-910. [Crossref] [Google Scholar]

23. Amiri M, et al. Magnetically retrievable ferrite nanoparticles in the catalysis application. Adv Colloid Interface Sci. 2019;271:101982. [Crossref] [Google Scholar] [PubMed]